Acta et Commentationes, Exact and Natural Sciences
Volume 21(1), 2026, Pages 18–28
UDC: 544.142.3:548.736:546.73:546.655

DOI: 10.36120/2587-3644.v21i1.18-28
ISSN: 2537-6284 E-ISSN: 2587-3644

Pentanuclear pivalate cluster with a $\{Co(III)_2Ce(IV)_3\}$ core

Ecaterina Beleaev, Daniel Brüx, Paul Kögerler, and Svetlana G. Baca

Abstract. The reaction of cobalt(II) pivalate and cerium(III) chloride with triethanolamine in acetonitrile led to the formation of a new pentanuclear cluster with the formula $[Co_2Ce_3O_2(piv)_7(Htea)_2(tea)]\cdot 2.5CH_3CN\cdot H_2O$ (**1**) (where H_3tea = triethanolamine, Hpiv = pivalic acid). A single crystal X-ray diffraction analysis revealed that **1** consists of a heterometallic pentanuclear assembly with a mixed-valent $\{Co_2Ce_3\}$ metal core composed of two Co(III) and three Ce(IV) ions. The metal atoms in **1** are connected by μ_3-O and μ_4-O oxo-bridges surrounded by seven pivalate groups. In addition, two partially deprotonated $Htea^{2-}$ and one fully deprotonated tea^{3-} ligands unite the metal atoms. The outer coordination sphere includes one water and two and a half acetonitrile molecules. The influence of the various types of intermolecular interactions between clusters and solvent molecules on the crystal packing in this system was evaluated using Hirshfeld surface analysis and 2D fingerprint plots.
Keywords: cobalt, cerium, triethanolamine ligand, coordination cluster, X-ray measurements, Hirshfeld surface analysis

Clusterul pentanuclear de pivalat cu un nucleu $\{Co(III)_2Ce(IV)_3\}$

Rezumat. Reacția pivalatului de cobalt(II) și a clorurii de ceriu(III) cu trietanolamină în acetonitril a condus la formarea unui nou cluster pentanuclear cu formula $[Co_2Ce_3O_2(piv)_7(Htea)_2(tea)]\cdot 2.5CH_3CN\cdot H_2O$ (**1**) (unde: H_3tea = trietanolamină, Hpiv = acid pivalic). Un studiu de difracție cu raze X pe monocristal a arătat că **1** constă într-o ansamblare pentanucleară heterometalică cu un miez metalic $\{Co_2Ce_3\}$, compus din doi ioni de Co(III) și trei ioni de Ce(IV). Atomii metalici din **1** sunt conectați prin punți oxo μ_3-O și μ_4-O înconjurate de șapte grupări pivalat. În plus, doi liganzi $Htea^{2-}$ parțial deprotonați și unul tea^{3-} complet deprotonat unesc atomii metalici. Sfera de coordinare exterioară include o moleculă de apă și două molecule și jumătate de acetonitril. Influența diferitelor tipuri de interacțiuni intermoleculare dintre clustere și moleculele de solvent asupra împachetării cristalelor în acest sistem a fost evaluată folosind analiza suprafeței Hirshfeld și grafice de amprentă 2D.
Cuvinte-cheie: cobalt, ceriu, ligand de trietanolamină, cluster de coordinare, măsurători cu raze X, analiza suprafației Hirshfeld

1. Introduction

Polynuclear heterometallic Ce-3d coordination compounds continue to attract considerable attention due to their potential use as electrocatalysts for oxygen and hydrogen evolution reactions [1], [2]. These compounds also find applications in a variety of other catalytic and industrial processes, including CO_2 reduction reactions and the conversion of CO_2 into biodegradable and biocompatible polycarbonate materials [3]. Ce-3d hybrid systems are also receiving attention due to their potential for designing and fabricating single-molecule magnets (SMMs) [4], [5]. However, mixed Ce-Co coordination compounds are rare, and only a few have been characterized in recent years [6], [7], [8], all of which having polymeric metal-organic framework (MOF) structures. For Ce-Co coordination compounds with discrete structures, a search of the Cambridge Structural Database [9] revealed 13 entries containing Ce(III) ions and featuring dinuclear $\{CoCe\}$ [10]-[13], trinuclear $\{Co_2Ce\}$ [14]-[18], tetranuclear $\{Co_3Ce\}$ [19], [20], and the biggest pentanuclear $\{Co_3Ce_2\}$ [21] cores. It should be note, that the combination of Ce(IV) and Co(II) or Co(III) ions is uncommon and only one heterometallic pentanuclear cluster with Ce(IV) ions having $\{Co_2^{III}Ce_3^{IV}\}$ core, $[Co_2^{III}Ce_3^{IV}O_2(L)(Me_3CCO_2)_6(bdea)_2]$ (where L = bicine), has been reported [22].

In continuation of our research on the preparation of homometallic Co(II,III) and heterometallic Co(II,III)-4f coordination clusters [23]-[26] we report here the synthesis of a new pentanuclear heterometallic compound with the formula $[Co_2^{III}Ce_3^{IV}O_2(piv)_7(Htea)_2(tea)]\cdot 2.5CH_3CN\cdot H_2O$ (**1**) (where H_3tea = triethanolamine, Hpiv = pivalic acid). The structure of **1** was determined by a single-crystal X-ray diffraction analysis. Furthermore, Hirshfeld surface analysis [27]-[29] was performed to qualitatively and quantitatively investigate the contributions of different types of intermolecular contacts to the crystalline packing.

2. Results and discussion

The pentanuclear cluster $[Co_2Ce_3O_2(piv)_7(Htea)_2(tea)]\cdot 2.5CH_3CN\cdot H_2O$ (**1**) was synthesized using a one-step self-assembly method, starting from cobalt(II) pivalate and cerium(III) chloride heptahydrate precursors. The reaction of a mixture of the above-mentioned salts with triethanolamine in acetonitrile solution under reflux conditions yielded cluster **1**. A single crystal X-ray diffraction analysis revealed that compound **1** crystallizes in the triclinic P-1 space group with the following unit cell parameters: a = 13.928(3) Å, b = 17.153(3) Å, c = 18.071(4) Å, α = 95.85(3)°, β = 109.59(3)°, γ = 95.98(3)°, and V = 4002.1(16) Å^3 (Table 1). Compound **1** consists of a heterometallic

pentanuclear cluster with a mixed-valent $\{Co_2^{III}Ce_3^{IV}\}$ core and solvent water and acetonitrile molecules (Figure 1). The formation of the mixed-valent core $\{Co_2^{III}Ce_3^{IV}\}$ is driven by the *in situ* oxidation of Co(II) to Co(III) and Ce(III) to Ce(IV). This oxidation is facilitated by the basic environment provided by the triethanolamine ligand and the presence of atmospheric oxygen. The cluster core in **1** is organized around a central trinuclear $\{Ce_3(\mu_3\text{-O})(\mu_4\text{-O})\}$ unit. In this arrangement, the μ_3-O (O1) and μ_4-O (O2) oxo-bridges facilitate the coordination of two Co(III) centers to the cerium(IV) framework (Figure 1b). Further, four pivalate moieties and two $Htea^{2-}$ ligands additionally link Co(III) centers with the $\{Ce_3O_2\}$ triangle. The metal centers within the $\{Ce_3O_2\}$ triangle motif are further stabilized by a bridging O atom from a piv^- group and two O atoms from fully deprotonated tea^{3-} ligand with Ce1···Ce2, Ce2···Ce3, and Ce1···Ce3 separations of 3.670(1), 3.810(1) and 3.732(1) Å, respectively. The remaining pivalates in a chelating manner satisfied the coordination sphere of Ce atoms. The Co–Ce distances vary between 3.218(1) and 5.811(2) Å, specifically 3.218(1), 3.235(1), 3.306(2), 3.337(1), 3.889(1), and 5.811(2) Å, whereas the Co···Co separation is 5.472(2) Å.

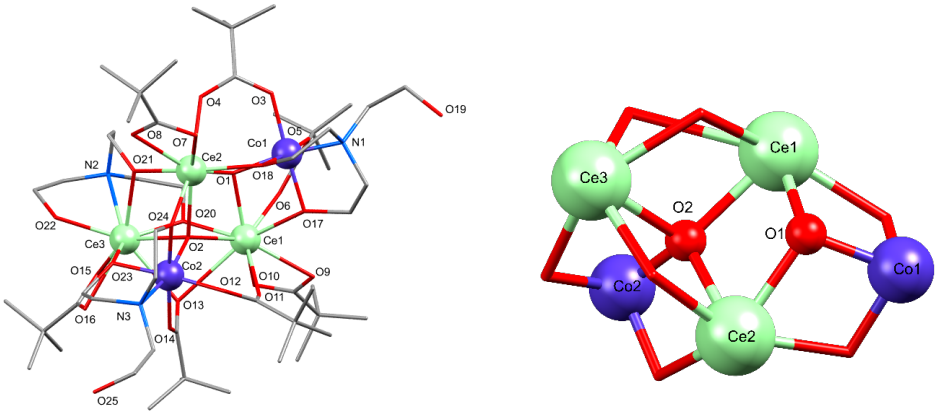

(a) (b)

Figure 1. Structure of **1** with a partial labeling scheme (a) and the $\{Co_2Ce_3\}$ metal core (b). Hydrogen atoms and solvate molecules are omitted for clarity

In **1**, the Co1 and Co2 centers display an octahedral NO_5 coordination environment defined by an oxo oxygen atom (μ_3-O atom for Co1 and μ_4-O atom for Co2), two oxygen atoms from two bridging piv^-, and two oxygen and nitrogen donor atoms from the $Htea^{2-}$ ligand. The Co–O bond distances are in the range 1.862(3)–1.930(3) Å, and the Co–N bond distances are 1.987(3) and 1.997(3) Å. Continuous shape measures (CShM)

calculated using the SHAPE program [30], [31] yield deviation values of 0.398 and 0.501 for the octahedral geometry (*OC-6*), confirming a slight distortion for Co1 and Co2, respectively (Table 3). The Ce1 center exhibits a nine-coordinate O_9 environment with a muffin geometry (*MFF-9*, CShM value 1.814), while the Ce2 center features an eight-coordinate O_8 environment (Figure 1), best described as a biaugmented trigonal prism geometry (*BTPR-8*, CShM value 3.167) (Table 3).

The coordination sphere of Ce1 is composed of μ_3-O and μ_4-O oxo ligands, two oxygen atoms from a chelating pivalate, three oxygen atoms from three bridging carboxylates, and two oxygen atoms from two $Htea^{2-}$ ligands. In contrast, for Ce2, the μ_3-O atom does not participate in coordination, resulting in an O_8 environment. The Ce1/Ce2-O bond distances range from 2.230(3) to 2.844(3) Å (Table 2). The Ce3 atom adopts a spherical capped square antiprism NO_8 coordination environment (*CSAPR-9*, CShM value 1.819), formed by a μ_4-oxo ligand, two oxygen atoms from chelating piv^-, one oxygen atom from a bridging pivalate, three oxygen and one nitrogen atoms from tea^{3-}, and oxygen atom from $Htea^{2-}$. The Ce3–O bond distances are in the range 2.241(3)-2.540(3) Å and Ce–N bond distance is 2.665(4) Å (Table 2).

Table 1. Crystal data and details of structural determinations for **1**

Formula	$C_{60}H_{112}Ce_3Co_2N_{5.50}O_{26}$
M_r g/mol^{-1}	1864.76
Crystal system	Triclinic
Space group	*P*-1
a/Å	13.928(3)
b/Å	17.153(3)
c/Å	18.071(4)
α/°	95.85(3)
β/°	109.59(3)
γ/°	95.98(3)
V/Å^3	4002.1(16)
Z	2
Final R_1, wR_2 (%)	0.0295, 0.0809
R indices R_1, wR_2 (all data) (%)	0.0373, 0.0873

Table 2. Interatomic distances (Å) for **1**

Ce(1)-O(1)	2.190(3)	Ce(2)-O(24)	2.314(3)	Ce(3)-N(2)	2.665(4)
Ce(1)-O(2)	2.318(3)	Ce(2)-O(4)	2.372(3)	Ce(3)-Co(2)	3.3066(17)
Ce(1)-O(17)	2.341(3)	Ce(2)-O(8)	2.461(3)	Co(1)-O(17)	1.864(3)
Ce(1)-O(20)	2.367(3)	Ce(2)-O(7)	2.493(3)	Co(1)-O(18)	1.880(3)
Ce(1)-O(11)	2.372(3)	Ce(2)-Co(1)	3.2181(9)	Co(1)-O(1)	1.885(3)
Ce(1)-O(6)	2.416(3)	Ce(2)-Co(2)	3.3371(9)	Co(1)-O(5)	1.913(3)
Ce(1)-O(10)	2.422(4)	Ce(2)-Ce(1)	3.6701(9)	Co(1)-O(3)	1.930(3)
Ce(1)-O(9)	2.513(3)	Ce(3)-O(22)	2.241(3)	Co(1)-N(1)	1.987(3)
Ce(1)-O(13)	2.845(3)	Ce(3)-O(20)	2.311(3)	Co(2)-O(24)	1.885(3)
Ce(1)-Co(1)	3.2349(11)	Ce(3)-O(23)	2.322(3)	Co(2)-O(23)	1.891(3)
Ce(1)-Ce(3)	3.7319(9)	Ce(3)-O(21)	2.339(3)	Co(2)-O(2)	1.911(3)
Ce(2)-O(1)	2.230(3)	Ce(3)-O(2)	2.425(3)	Co(2)-O(12)	1.917(3)
Ce(2)-O(21)	2.274(3)	Ce(3)-O(15)	2.479(3)	Co(2)-O(14)	1.922(3)
Ce(2)-O(2)	2.284(3)	Ce(3)-O(16)	2.485(3)	Co(2)-N(3)	1.997(3)
Ce(2)-O(18)	2.301(3)	Ce(3)-O(13)	2.540(3)		

The Hirshfeld molecular surfaces for the neutral $[Co_2Ce_3O_2(piv)_7(Htea)_2(tea)]$ cluster in **1** was generated at high resolution, with the three-dimensional surface mapped over d_{norm} using a fixed color scale from −0.6969 to +1.5695 [27] (Figure 2a). Two-dimensional (2D) fingerprint plots [28], [29] were utilized to quantify the contributions of all intermolecular contacts (Figure 2b). Analysis reveals that H$\cdots$H interactions are predominant, accounting for 82.9% of the Hirshfeld surface and reflecting their dominance in the crystal packing. In addition, O$\cdots$H/H$\cdots$O and N$\cdots$H/H$\cdots$N interactions, associated with hydrogen bonding, contribute 6.4% and 7.7%, respectively. These contacts appear as characteristic sharp spikes in the fingerprint plots, arising from the presence of carboxylate groups and hydroxyl functionalities associated with the triethanolamine ligand and solvate molecules.

Table 3. Continuous shape measures (CShM) of the coordination geometries of metal centers in **1** using SHAPE v2.0 [30]*

	JPPY-6	*TPR*-6	*OC*-6	*PPY*-6	*HP*-6
ML6	Johnson pentagonal pyramid J2 (C_{5v})	Trigonal prism (D_{3h})	Octahedron (O_h)	Pentagonal pyramid (C_{5v})	Hexagon (D_{6h})
Co1	30.645	13.823	**0.398**	26.537	32.002
Co2	29.006	13.476	**0.501**	25.062	31.960

	ML8	Ce2		*ML9*	Ce1	Ce3
ETBPY-8	Elongated trigonal bipyramid (D_{3h})	22.477	*MFF-9*	Muffin (C_s)	**1.814**	2.152
TT-8	Triakis tetrahedron (T_d)	11.036	*HH-9*	Hula-hoop (C_{2v})	7.693	10.495
JSD-8	Snub disphenoid (J84) (D_{2d})	4.323	*JTDIC-9*	Tridiminished icosahedron (J63) (C_{3v})	13.058	12.207
BTPR-8	Biaugmented trigonal prism (C_{2v})	**3.167**	*TCTPR-9*	Tricapped trigonal prism (D_{3h})	2.650	1.894
JBTPR-8	Johnson - Biaugmented trigonal prism (J50) (C_{2v})	3.851	*JTCTPR-9*	Tricapped trigonal prism (J51) (D_{3h})	3.306	2.037
JETBPY-8	Johnson - Elongated triangular bipyramid (J14) (D_{3h})	26.415	*CSAPR-9*	Capped square antiprism (C_{4v})	1.890	**1.819**
JGBF-8	Johnson - Gyrobifastigium (J26) (D_{2d})	8.495	*JCSAPR-9*	Capped sq. antiprism (C_{4v})	3.184	2.228
TDD-8	Triangular dodecahedron (D_{2d})	3.557	*CCU-9*	Capped cube (C_{4v})	8.544	7.309
SAPR-8	Square antiprism (D_{4d})	5.093	*JCCU-9*	Capped cube (Elongated square pyramid, J8) (C_{4v})	8.907	7.972
CU-8	Cube (O_h)	10.210	*JTC-9*	Triangular cupola (J3) (C_{3v})	14.439	13.291
HBPY-8	Hexagonal bipyramid (D_{6h})	10.617	*HBPY-9*	Heptagonal bipyramid (C_{7v})	16.673	17.446
HPY-8	Heptagonal pyramid (C_{7v})	21.855	*OPY-9*	Octagonal pyramid (C_{8v})	20.509	22.501
OP-8	Octagon (D_{8h})	29.995	*EP-9*	Enneagon (D_{9h})	32.122	31.811

* A value of zero corresponds to an exact match of the corresponding center to the ideal geometry.

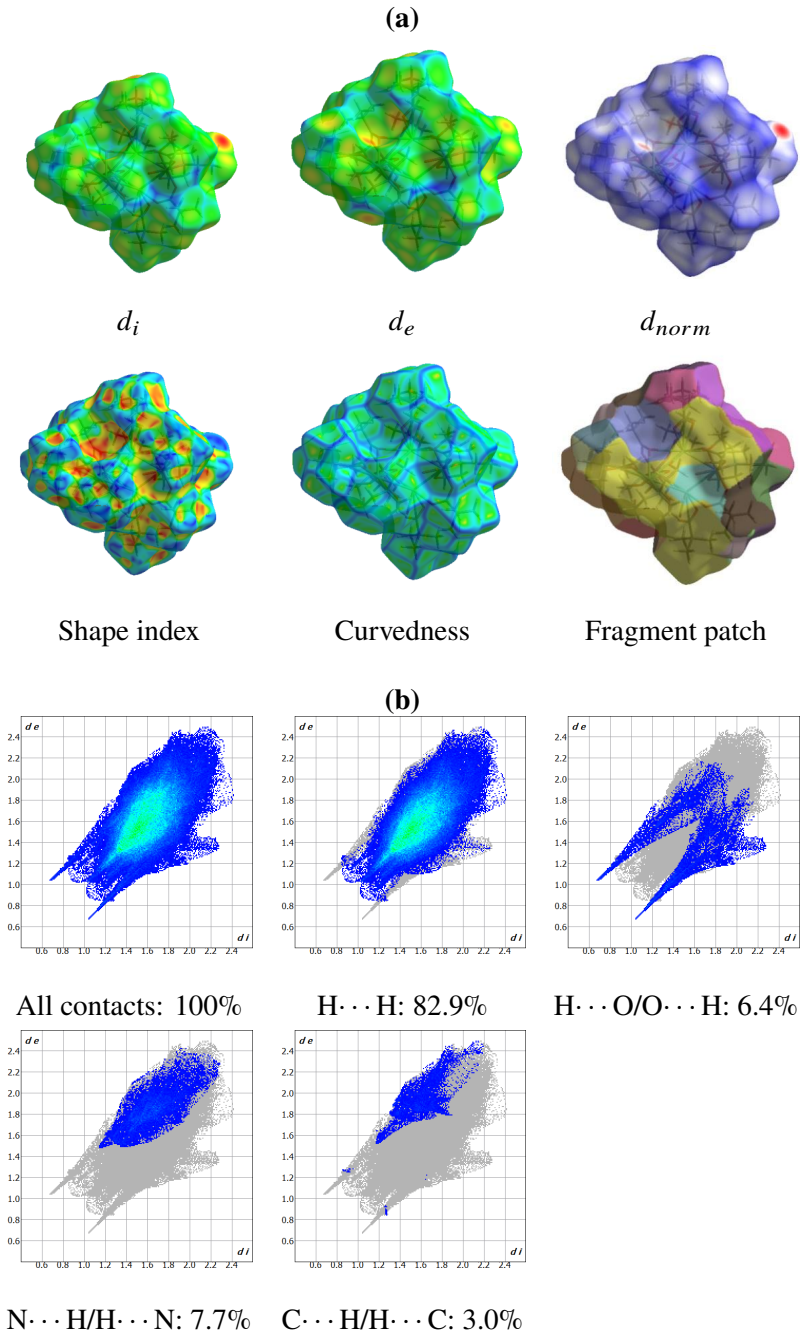

Figure 2. View of the Hirshfeld surface for the $[Co_2Ce_3O_2(piv)_7(Htea)_2(tea)]$ cluster decorated with different properties (a) and 2D fingerprint plots (d_e vs. d_i) for all and individual contacts in crystal packing of **1** (b)

3. Conclusion

In summary, the novel pentanuclear heterometallic cluster $[Co_2Ce_3O_2(piv)_7(Htea)_2(tea)]\cdot 2.5CH_3CN\cdot H_2O$ (**1**) was successfully synthesized and characterized. Structural analysis revealed a unique $\{Co(III)_2Ce(IV)_3O_2\}$ core architecture, in which cobalt(III) and cerium(IV) ions are linked by oxo groups, pivalate bridges and deprotonated triethanolamine ligands. Additionally, Hirshfeld surface analysis provided valuable quantitative insights into the intermolecular interactions, thereby validating the structural stability and packing of the assembly. These results provide further insight into the structural chemistry of Co-4f clusters and highlight the role of carboxylate and polyalcohol ligands in governing their supramolecular assembly.

Acknowledgements. *The authors are grateful for the subprogram 011202 financed by the Ministry of Education and Research of R. Moldova and the bilateral project "MultiClust" (01DK25013 and 25.80013.5007.07GER) supported by the German Federal Ministry of Education and Research (BMBF).*

References

[1] SHI, J.; BAO, Y.; YE, R.; ZHONG, J.; ZHOU, L.; ZHAO, Z.; KANG, W.; AIDAROVA, S.B. Recent progress and perspective of electrocatalysts for the hydrogen evolution reaction. *Catalysis Science & Technology*. 2025, vol. 15, pp. 2104–2131. DOI: 10.1039/D4CY01449A.

[2] INAMDAR, A.I.; SALUNKE, A.S.; SEOK, J.H.; CHAVAN, H.S.; SHRESTHA, N.K.; LEE, S.U.; CHO, S. and IM, H. Cobalt oxide/cerium oxide heterogeneous interfaces as advanced durable and bifunctional electrocatalysts for robust industrially relevant overall water splitting. *Journal of Materials Chemistry A*. 2024, vol. 12, pp. 31362–31374. DOI: 10.1039/D4TA05895J.

[3] YARI, F.; ALJABOUR, A.; AWADA, H.; MICHALKE, J.; KUMARI, N.; COSKUN-ALJABOUR, H.; ROY, S.; KRISCH, D. and SCHÖFBERGER, W. Synergistic Interactions in a Heterobimetallic Ce (III)–Ni (II) Diimine Complex: Enhancing the Electrocatalytic Efficiency for CO_2 Reduction. *ACS Applied Energy Materials*. 2024, vol. 7, no. 21, pp. 10052–10060. DOI: `https://doi.org/10.1021/acsaem.4c02132`.

[4] LIU, K.; SHI, W. and CHENG, P. Toward heterometallic single-molecule magnets: Synthetic strategy, structures and properties of 3d–4f discrete complexes. *Coordination Chemistry Reviews*. 2015, vol. 289, pp. 74–122. DOI: 10.1016/j.ccr.2014.10.004.

[5] MISHRA, A.; TASIOPOULOS, A.J.; WERNSDORFER, W.; MOUSHI, E.E.; MOULTON, B.; ZAWOROTKO, M.J.; ABBOUD, K.A. and CHRISTOU, G. Single-molecule magnets: a family of Mn^{III}/Ce^{IV} complexes with a $[Mn_8CeO_8]^{12+}$ core. *Inorganic Chemistry*. 2008, vol. 47, no. 11, pp. 4832–4843. DOI: 10.1021/ic8001064.

[6] MA, S.; SHI, Y.; XIA, X.; SONG, Q. AND YANG, J. Cerium-cobalt bimetallic metal–organic frameworks with the mixed ligands for photocatalytic degradation of methylene blue. *Inorganic Chemistry Communications*. 2023, vol. 152, p. 110664. DOI: 10.1016/j.inoche.2023.110664.

[7] ZHU, G.; TAN, J.; TAN, L.; WU, Q.; REN, X.; FU, C.; CHEN, Z. AND MENG, X. Growth of CeCo-MOF in dendritic mesoporous organosilica as highly efficient antioxidant for enhanced thermal stability of silicone rubber. *Chinese Chemical Letters*. 2025, vol. 36, no. 1, p. 109669. DOI: 10.1016/j.cclet.2024.109669.

[8] SUN, P.-P.; DENG, S.-P.; LI, J.-Q.; WU, X.; ZHANG, Y.-F.; LIU, H.-Y. AND SHI, F.-N. A MOF-derived flower-shaped CeCo-oxide as a multifunctional material for high-performance lithium-ion batteries and supercapacitors. *Journal of Colloid and Interface Science*. 2024, vol. 661, pp. 564–573. DOI: 10.1016/j.jcis.2024.01.196.

[9] GROOM, C.R.; BRUNO, I.J.; LIGHTFOOT, M.P. AND WARD, S.C. The Cambridge Structural Database. *Acta Crystallographica Section B*. 2016, vol. 72, pp. 171–179. DOI: 10.1107/S2052520616003954.

[10] COLLINS, T.J. AND WORKMAN, J.M. Structure of tetraphenylphosphonium μ-$\{\eta^4$-2,4-bis(2-hydroxy-2-methylpropanamido)-2,4-dimethyl-3-oxopentane$\}$cobalt(III) tetranitratocerium(III) dichloromethane. *Acta Crystallographica Section C: Crystal Structure Communications*. 1993, vol. 49, pp. 1426–1428. DOI: 10.1107/S0108270193002161.

[11] SCHWOB, T.; KUNNAS, P.; JONGE, N.; PAPP, C.; STEINRÜCK, H.-P. AND KEMPE, R. General and selective deoxygenation by hydrogen using a reusable earth-abundant metal catalyst. *Science Advances*. 2019, vol. 5, p. eaav3680. DOI: 10.1126/sciadv.aav3680.

[12] ELIAS, J.S.; RISCH, M.; GIORDANO, L.; MANSOUR, A.N. AND SHAO-HORN, Y. Structure, bonding, and catalytic activity of monodisperse, transition-metal-substituted CeO_2 nanoparticles. *Journal of the American Chemical Society*. 2014, vol. 136, pp. 17193–17200. DOI: 10.1021/ja509214d.

[13] KLAUSFELDER, B.; BLACH, P.; JONGE, N. AND KEMPE, R. Synthesis of 3,4-dihydro-2*H*-pyrroles from ketones, aldehydes, and nitro alkanes via hydrogenative cyclization. *Chemistry – A European Journal*. 2022, vol. 28, p. e202201307. DOI: 10.1002/chem.202201307.

[14] AHMED, N. AND ANSARI, K.U. Experimental and theoretical insights into Co–Ln magnetic exchange and the rare slow-magnetic relaxation behavior of $[Co^{II}_2Pr]^{2+}$ in a series of linear $[Co^{II}_2Ln]^{2+}$ complexes. *Dalton Transactions*. 2022, vol. 51, pp. 4122–4234. DOI: 10.1039/D1DT03573H.

[15] HOSSAIN, M.S.; MITSUHASHI, R.; IMAI, Y. AND HAYASHI, Y. Synthesis, structure, and magnetic properties of lanthanide(III) complexes incorporating a tris-chelate cobalt(III) complex as a metalloligand. *Journal of Coordination Chemistry*. 2024, vol. 77, no. 12-14, pp. 1489–1499. DOI: 10.1080/00958972.2024.2369132.

[16] TRIEU, T.N.; NGUYEN, M.H.; ABRAM, U. AND NGUYEN, H.H. Syntheses and structures of new trinuclear $M^{II}LnM^{II}$ (M = Ni, Co; Ln = Gd, Ce) complexes with 2,6-bis(acetobenzoyl)pyridine. *Zeitschrift für Anorganische und Allgemeine Chemie*. 2015, vol. 641, pp. 863–870. DOI: 10.1002/zaac.201500016.

[17] JESUDAS, J.J.; PHAM, C.T.; HAGENBACH, A.; ABRAM, U. AND NGUYEN, H.H. Trinuclear $Co^{II}Ln^{III}Co^{II}$ complexes (Ln = La, Ce, Nd, Sm, Gd, Dy, Er, and Yb) with 2,6-dipicolinoylbis(*N*,*N*-diethylthiourea): synthesis, structures, and magnetism. *Inorganic Chemistry*. 2020, vol. 59, pp. 386–395. DOI: 10.1021/acs.inorgchem.9b02648.

[18] PU, L.-M.; ZHAO, Q.; LIU, L.-Z.; ZHANG, H.; LONG, H.-T. AND DONG, W.-K. Synthesis and fluorescence properties of a new heterotrinuclear Co(II)-Ce(III)complex constructed from a bis(salamo)-type tetraoxime ligand. *Molecules*. 2018, vol. 23, p. 804. DOI: 10.3390/molecules23040804.

[19] LIU, Y.; SHI, D. AND XU, F. Design of molecular magnetic materials based on a new family of mixed-lanthanide Co-Ln clusters by the use of the 1,3-bis[*tris*(*hydroxymethyl*)-*methylamino*]propane ligand. *Polyhedron*. 2022, vol. 217, p. 115754. DOI: 10.1016/j.poly.2022.115754.

[20] ASABA, H.; IWASAKI, T.; HATAZAWA, M.; DENG, J.; NAGAE, H.; MASHIMA, K. AND NOZAKI, K. Alternating copolymerization of CO_2 and cyclohexene oxide catalyzed by cobalt–lanthanide mixed multinuclear complexes. *Inorganic Chemistry*. 2020, vol. 59, pp. 7928–7933. DOI: 10.1021/acs.inorgchem.0c01156.

[21] GAO, S.; BAI, O.; MA, B.-Q.; YI, T.; YAN, C.-H. AND XU, G.-X. A novel two-dimensional 4f-3d coordination polymer $Ce_2Co_3(EDTA)_3(H_2O)_{11}\cdot 12H_2O$. *Journal of Chemical Crystallography*. 2000, vol. 30, pp. 163–166. DOI: 10.1023/A:1009574829495.

[22] SEISS, M.; LORENZ, J.; SCHMITZ, S.; MOORS, M.; BÖRNER, M.; MONAKHOV, K.Y. Synthesis and structures of cobalt-expanded zirconium- and cerium-oxo clusters as precursors for mixed-metal oxide thin films. *Dalton Transactions*. 2024, vol. 53, pp. 8454–8462. DOI: 10.1039/D4DT00328D.

[23] STATI, D.; VAN LEUSEN, J.; KRAVTSOV, V.CH.; CHUMAKOV, Y.; KÖGERLER, P. AND BACA, S.G. Variations of heterometallic cores and magnetic properties in Co(III)–Y/Ln isobutyrate clusters with *N*-butyldiethanolamine: from tetranuclear to octanuclear clusters. *RSC Advances*. 2025, vol. 15, no. 23, pp. 18209–18223. DOI: 10.1039/d5ra02513c.

[24] STATI, D.; VAN LEUSEN, J.; KRAVTSOV, V.CH.; KRÄMER, K.W.; LIU, SH.-X.; DECURTINS, S.; KÖGERLER, P. AND BACA, S.G. Hexadecanuclear isobutyrate nanoclusters with a $\{Co^{II}_{14}Co^{III}_{2}\}$ core. *CrystEngComm*. 2024, vol. 26, no. 32, pp. 4264–4271. DOI: 10.1039/D4CE00637B.

[25] STATI, D.; VAN LEUSEN, J.; AHMED, N.; KRAVTSOV, V.CH.; KÖGERLER, P. AND BACA, S.G. A $\{Co^{III}_{2}Dy^{III}_{4}\}$ single-molecule magnet with an expanded core structure. *Crystal Growth & Design*. 2023, vol. 23, no. 1, pp. 395–402. DOI: 10.1021/acs.cgd.2c01085.

[26] BELEAEV, E.; KRAVTSOV, V. AND BACA, S. Heterometallic tetranuclear $\{Co(III)_2Ln(III)_2\}$ coordination complexes based on pivalate and N-butyldiethanolamine ligands. In: *Materials Science and Condensed Matter Physics*, 2024, pp. 96–96.

[27] WOLFF, S.K.; GRIMWOOD, D.J.; MCKINNON, J.J.; TURNER, M.J.; JAYATILAKA, D. AND SPACKMAN, M.A. CrystalExplorer: a program for Hirshfeld surface analysis, visualization and quantitative analysis of molecular crystals. *Journal of Applied Crystallography*. 2021, vol. 54, pp. 1006–1011. DOI: 10.1107/S1600576721002910.

[28] HIRSHFELD, F.L. Bonded-atom fragments for describing molecular charge densities. *Theoretica Chimica Acta*, 1977, vol. 44, pp. 129–138. DOI: 10.1007/BF00549096.

[29] SPACKMAN, M.A. AND JAYATILAKA, D. Hirshfeld surface analysis. *CrystEngComm*. 2009, vol. 11, pp. 19–32. DOI: 10.1039/B818330A.

[30] LLUNELL, M.; CASANOVA, D.; CIRERA, J.; BOFILL, J.M.; ALEMANY, P.; ALVAREZ, S.; PINSKY, M. AND AVNIR, D. *SHAPE: Continuous shape measures of polygonal and polyhedral molecular fragments*. Barcelona: University of Barcelona, 2005.

[31] ALVAREZ, S.; ALEMANY, P.; CASANOVA, D.; CIRERA, J.; LLUNELL, M. AND AVNIR, D. Shape maps and polyhedral interconversion paths in transition metal chemistry. *Coordination Chemistry Reviews*. 2005, vol. 249, no. 17-18, pp. 1693–1708. DOI: 10.1016/j.ccr.2005.03.031.

Received: April 17, 2026 *Accepted: July 15, 2026*

(Ecaterina Beleaev, Svetlana G. Baca) INSTITUTE OF APPLIED PHYSICS, MOLDOVA STATE UNIVERSITY, CHIȘINĂU, REPUBLIC OF MOLDOVA
https://orcid.org/0000-0003-0266-5316, https://orcid.org/0000-0002-2121-2091
E-mail address: ecaterina.beleaev@ifa.usm.md, svetlana.baca@ifa.usm.md

(Daniel Brüx, Paul Kögerler) INSTITUTE OF INORGANIC CHEMISTRY, RWTH AACHEN UNIVERSITY, AACHEN, GERMANY
https://orcid.org/0009-0008-1483-2859, https://orcid.org/0000-0001-7831-3953
E-mail address: daniel.bruex@rwth-aachen.de, paul.koegerler@ac.rwth-aachen.de